Computers and Concrete, *Vol. 15, No. 5 (2015) 771-794*
DOI: http://dx.doi.org/10.12989/cac.2015.15.5.771

Selection of measurement sets in static structural identification of bridges using observability trees

Jose Antonio Lozano-Galant[*1], Maria Nogal[2a], Jose Turmo[3b] and Enrique Castillo[4c]

[1]*Department of Civil Engineering, University of Castilla-La Mancha, Ciudad Real, Spain*
[2]*Department of Civil, Structural and Environmental Engineering, Trinity College, Dublin, Ireland*
[3]*Department of Construction Engineering,*
Universitat Politècnica de Catalunya BarcelonaTECH, Barcelona, Spain
[4]*Department of Applied Mathematics and Computational Sciences, University of Cantabria, Santander, Spain*

(Received August 27, 2014, Revised January 8, 2015, Accepted January 16, 2015)

Abstract. This paper proposes an innovative method for selection of measurement sets in static parameter identification of concrete or steel bridges. This method is proved as a systematic tool to address the first steps of Structural System Identification procedures by observability techniques: the selection of adequate measurement sets. The observability trees show graphically how the unknown estimates are successively calculated throughout the recursive process of the observability analysis. The observability trees can be proved as an intuitive and powerful tool for measurement selection in beam bridges that can also be applied in complex structures, such as cable-stayed bridges. Nevertheless, in these structures, the strong link among structural parameters advises to assume a set of simplifications to increase the tree intuitiveness. In addition, a set of guidelines are provided to facilitate the representation of the observability trees in this kind of structures. These guidelines are applied in bridges of growing complexity to explain how the characteristics of the geometry of the structure (e.g. deck inclination, type of pylon-deck connection, or the existence of stay cables) affect the observability trees. The importance of the observability trees is justified by a statistical analysis of measurement sets randomly selected. This study shows that, in the analyzed structure, the probability of selecting an adequate measurement set with a minimum number of measurements at random is practically negligible. Furthermore, even bigger measurement sets might not provide adequate SSI of the unknown parameters. Finally, to show the potential of the observability trees, a large-scale concrete cable-stayed bridge is also analyzed. The comparison with the number of measurements required in the literature shows again the advantages of using the proposed method.

Keywords: bridge; structural system identification; observability trees; damage detection; measurement set

*Corresponding author, Ph.D., E-mail: joseantonio.lozano@uclm.es
[a] Ph.D., E-mail: nogalm@tcd.ie
[b] Ph.D., E-mail: jose.turmo@upc.edu
[c] Ph.D., E-mail: enrique.castillo@unican.es

http://www.techno-press.org/?journal=cac&subpage=8 ISSN: 1598-8198 (Print), 1598-818X (Online)

1. Introduction

The structural response of a bridge is traditionally based on simplistic physically based models (e.g. Finite Element Models, FEMs). Actual parameters of built structures (such as axial stiffness, E_jA_j, flexural stiffness, E_jI_j, area, A_j or inertia, I_j) might differ from those assumed in these FEMs. For this reason, calibration of the models is required for accurate and reliable estimation of stress distribution and deformations of built structures (see Turker *et al*. 2014). One way to approach this need is by using measurements from health monitoring system (see Ni *et al.* 2011). This process is known as Structural System Identification (SSI) (see ASCE 2011).

Adeli and Jiang (2006) classified the SSI methods as parametric (see Sanayei and Saletnik 1996), in which the set of equations has a physical meaning, and non-parametric (see Erdogan and Bakir 2013), in which it has not. According to the type of excitation, the SSI methods can also be classified as input-output methods or only output methods. The main difference between both groups refers to the information of the excitation loads. In the input-output method, the excitation loads might be assumed known while in the output-only methods they are unknown. Multiple examples of input-output methods have been presented in the literature for dynamic (see Arslan and Durmus 2013), static (see Lakshmanan *et al*. 2008, Ubertini *et al.* 2013) or mixed (see Lee *et al*. 2010) excitation. Static methods can identify only stiffness parameters and are not able to capture any changes in mass and damping parameters, while dynamic methods can identify changes in all structural parameters. Nevertheless, many applications require only element stiffness identification for condition assessment. In these cases, static methods can prove simpler and more adequate for economical and computational time reasons (see Sanayei *et al*. 1997).

In any SSI method, different measurement sets can be used to calculate the desired estimates. Often the number of deflections that can be measured in a structure is limited due to available funds, equipment, and/or accessibility conditions. Therefore, a key pretest decision for the SSI method is the selection of the minimum number of measurement points and their location for successful parameter estimation. Several authors have presented heuristic methods to select near-optimal measurement set from non-destructive static (see Sanayei *et al.* 1992) and dynamic (see Pothisiri and Hjelmstad 2002) structural responses. Meo and Zumpano (2005) compared different optimal sensor placement techniques. Zhang and Ohsaki (2011) proposed an optimization problem to search for the optimal set of locations for measurement of member forces to have the highest identification accuracy. Raich and Liszkai (2012) optimized both the number and location of dynamic sensors. Recently, Joshua and Varghese (2013) used decision trees to select the location of accelerometers in bricklayers.

Lozano-Galant *et al*. (2013a, 2014a) proposed the novel application of observability techniques to SSI in trusses, beams and frame structures and the validation of this methodology to deal with the peculiarities of cable-stayed bridges. This technique can be applied regardless of the load type. This comes from the fact that the observability technique is applied in the system of equations coming from the stiffness matrix method. The only restriction of the load test used in the observability technique is that it needs to excite the parameter to be estimated. For example, it is clear to notice that the flexural stiffness of one horizontal beam cannot be estimated when only a horizontal load is introduced, as this load does not excite the flexural mechanism. A hitch that impeded a practical application of the observability method was the fact that the measurement set selection was carried out by trial and error analysis, that is, without a systematic procedure. It is important to highlight that this selection is a crucial step in the SSI. Nevertheless, and despite its importance, no adequate procedure for measurement set selection by observability techniques has

been found in the literature. To fill this gap, the major contribution of the current paper is based on the definition of a systematic procedure for measurement set selection in SSI by observability techniques. The new systematic method presented in this paper corresponds with the observability trees technique.

The observability trees show graphically how the estimates are successively calculated (observability flow) throughout the recursive process of the observability analysis. The trees are defined by two different elements: tree nodes (unknown variables that correspond with unknown estimates, as stiffness, areas or inertias) and tree branches (information measured at the nodes of the structure, such as rotations or deflections). The aim of the method is to define an observability flow that enables the connection of the pursued tree nodes. To initiate an observability flow in these trees, the measured deflections must fulfill a set of requirements regarding both, deflection type and location. Finally, to propagate adequately the flow, the measured deflections must provide adequate connectivity to these nodes. Observability trees can also be used to look for alternative measurements if required.

It is important to highlight that the observability trees technique presented in this paper is a symbolic and parametric procedure in which the obtained results do not depend on the numerical values. For this reason, and in order to avoid unnecessary data, the numerical analyses have been intentionally omitted in the analyzed examples.

This paper is organized as follows. In Section 2, the concept of observability tree is presented for beam structures. After analyzing the effects of the structural redundancy and the beam inclination, an algorithm is described for measurement set selection in beams. In Section 3, the application of the observability trees in cable-stayed bridges is presented. A set of simplifications are provided to facilitate the representation of the observability trees of cable-stayed bridges. From these simplifications, a set of guidelines to make observability tress in cable-stayed bridges is presented. These guidelines are applied for measurement set selection of cable-stayed bridges of growing complexity. Furthermore, the effectiveness of random measurement set selection is also analyzed. Finally, in Section 4, some conclusions are drawn.

2. Observability trees

The observability trees are graphical representations that illustrate the connectivity of the unknown parameters (such as E_jA_j, E_jI_j, E_j, A_j or I_j) into the system of equations of the stiffness matrix method as well as the recursive process described in Lozano-Galant *et al.* (2013a, 2014a) and Castillo *et al.* (2014). These trees can be used for systematic measurement set selection in SSI by observability techniques.

In orthogonal grids, axial and flexural structural resistant mechanisms can be studied separately. Therefore, two different observability trees, referring to the axial (T_N) and flexural (T_M) resistant mechanism, can be analyzed independently of each other. On the contrary, in those cases where both resistant mechanisms are coupled together, as in inclined beams, these trees are joined in a common tree ($T_{N\text{-}M}$). Any observability tree is composed of two different elements: the tree nodes (represented by the unknown estimates, see Fig. 1) and straight lines called tree branches that connect the tree nodes (see Fig. 1). These branches represent the equation or equations that link unknown estimates in the stiffness matrix method. They also include the deflections and/or rotations measured at the corresponding nodes of the structure.

In horizontal beams, information of the axial resistant mechanism depends on the horizontal

deflections in nodes, u_k, while information of the flexural resistant mechanism depends on the vertical deflections, v_k, and the rotations, w_k, in structural nodes *k*. On the other hand, in vertical beams the role of the horizontal and vertical deflections is exchanged or swapped. The shape of the tree depends on the connectivity and beam elements inclination, the structural redundancy, the known and unknown structural parameters and the measured deformations.

To illustrate the definition of the observability trees from the stiffness matrix, the T_N and T_M trees of a horizontal continuous beam without boundary conditions are summarized in Fig. 1. The FEM of this beam includes 4 nodes and 3 beam elements (bars) L_1, L_2 and L_3 long, respectively. The contribution of each bar to the stiffness matrix of the structure is highlighted by a dashed line. The mechanical properties of the beam elements, that is, A_1, A_2, A_3, I_1, I_2 and I_3, are assumed as unknown. The Young's modulus, the length of all the beam elements and the forces in nodes (H_k, V_k and M_k) are assumed as known. The system of equations of the stiffness matrix includes 3 equations for each node of the structure. With k being the node number, the equations of the *kth* node are located between the row 3(k-1) + 1 and the row 3k of the stiffness matrix. The contribution of each structural node into the system of equations has been framed in the vectors of forces and displacements of Fig. 1. In this case, the axial resistant mechanism of the structure is represented by the horizontal deflections, u. This is to say, in the first equation of each node. These 4 equations are framed with continuous lines in Fig. 1. From these equations, the axial observability tree, T_N, can be directly represented. This tree includes three tree nodes (unknown areas in beam elements, A_1 to A_3) and four branches that refer to the 4 equations that link the tree nodes. These branches include information of the corresponding horizontal node deflections (u_1 to u_4). The flexural observability tree, T_M, can be obtained from the equations that represent the bending resistant mechanism of the structure. These equations are highlighted by a dotted line in Fig. 1. In this case, the T_M tree also includes three tree nodes (unknown inertias in beam elements, I_1 to I_3) and four branches. Each of these branches involves the two different equations that correspond to the equilibrium of vertical forces and moments in the corresponding node of the structure. Therefore, these branches might include information on the vertical deflections and/or rotations in the structural nodes (v_1 to v_4 and w_1 to w_4).

The observability trees can be used to define measurement sets with a minimum number of measurements. The number of required deflections, N_D, to estimate a structure with N_A unknown Areas or Axial stiffnesses and N_I unknown Inertias or bending stiffnesses can be expressed as

$$N_D = N_A + N_I \tag{1}$$

One of the advantages of identifying a minimum measurement set is that if this is done, a consistent system of equations is obtained. It is true that the estimates obtained in this system depend, to a great extent, on the accuracy of the monitored data. Nevertheless, either additional measurements or measurement repetitions might provide different consistent systems with different values of the estimates. Analysis of these estimates can be used to minimize the errors in estimates. It is remarked that if a minimum measurement set is not defined, an inconsistent system of equations can be obtained. This type of system cannot be appropriately solved with observability techniques. This proves the interest and the importance of the method presented in this paper.

In addition to the number of measurements, the type of deflection and its location are of primary importance. In fact, when the deflection types or the locations are not properly selected, even a higher number N_D does not enable the observability of the unknown estimates. The location and the type of measurement required to obtain the minimum set of deflections can be obtained by

the recursive process of the observability analysis. This process can be seen as an "observability flow" that shows how the equations of the stiffness matrix method are successively solved.

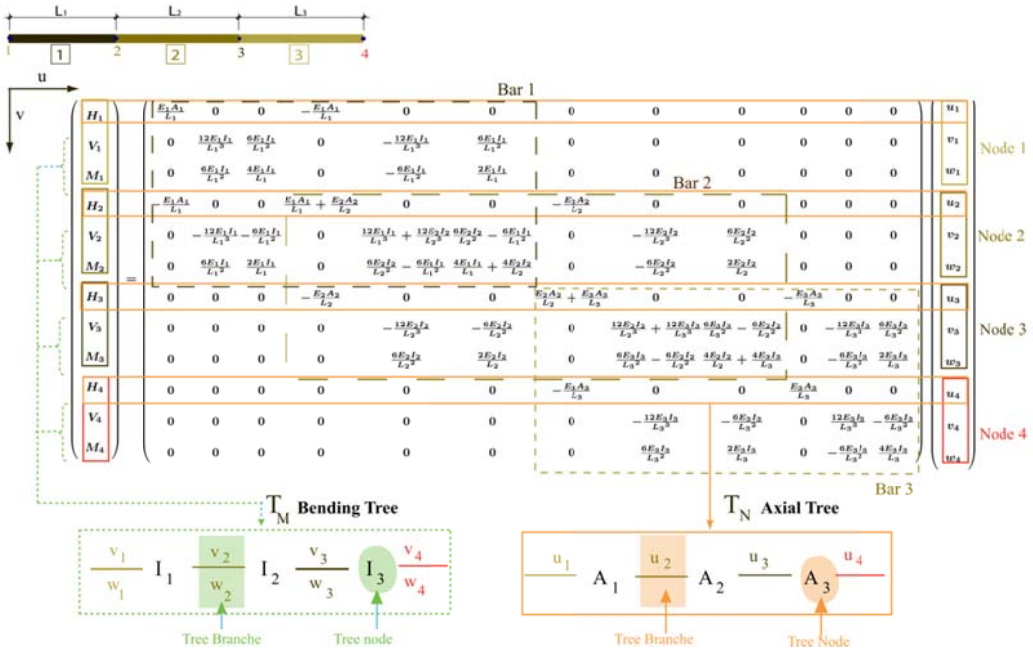

Fig. 1 Definition of the bending (T_M) and the axial (T_N) trees from the stiffness matrix

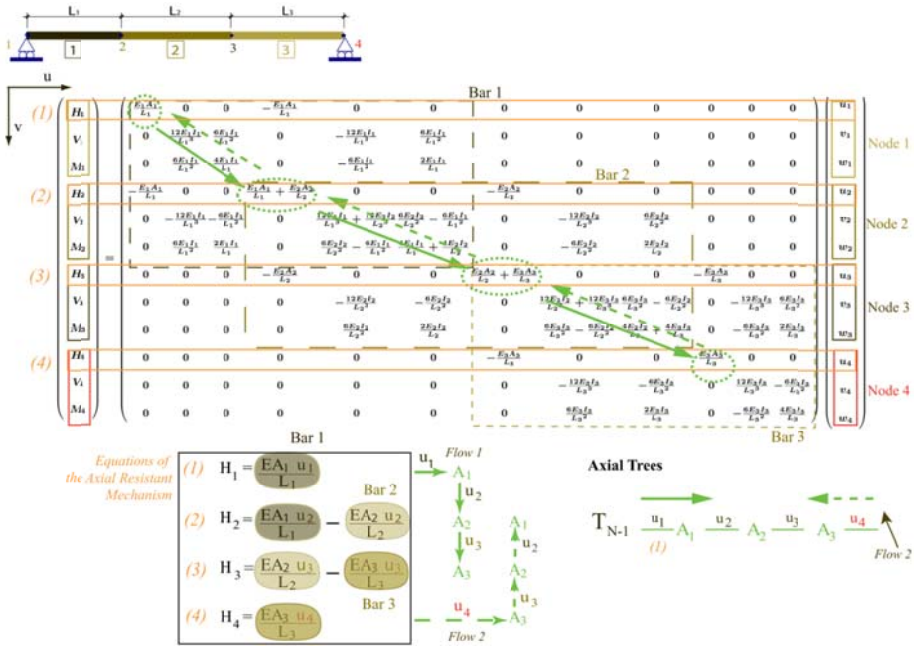

Fig. 2 Determination of observability flows from the stiffness matrix method

The observability flow starts when some parts of the structure include enough information to evaluate one or several unknown estimates. To propagate adequately the flow, the measured deflections in tree branches must provide adequate connectivity to the tree nodes. In this way, observed estimates together with measured deflections can be used to solve some equations in adjacent beam elements.

To illustrate the concept of observability flow and its role in the solution of the system of equations of the stiffness matrix method, let's focus on Fig. 2. This Fig. includes the system of equations of the stiffness matrix method for the continuous beam analyzed in Fig. 1. The 4 equations that govern the axial behavior of the structure are framed with a continuous line and numbered from (1) to (4) in Fig. 1.

To show how the connectivity of the beams links the equations of the axial resistant mechanism, equations are rewritten at the bottom of Fig. 2. In these equations, the terms referring to the axial stiffness of each beam are represented with a different color. For example, the axial stiffness of bar 1 appears in the equilibrium equations of its both nodes (Eqs. (1) and (2) of Fig. 1) while the axial stiffness of bar 2 appears in Eqs. (2) and (3) of Fig. 1. If the Young's modulus, the length of the bars and the horizontal forces in nodes (H_1 to H_4) are assumed as known and the areas of the bars are assumed as unknown, the equations of the axial resistant mechanism include 7 unknown variables (A_1 to A_3 and u_1 to u_4). Furthermore, unknown horizontal deflections and areas are multiplied making the problem nonlinear. To estimate the unknown areas (objective of the SSI), a set of horizontal deflections at the structural nodes is first measured. Measuring horizontal deflections of all structural nodes (that is, u_1 to u_4) leads to a system with more equations than unknown variables, which can be solved directly (assuming that one equation is redundant). Nevertheless, we can take advantage of the connectivity of the unknown estimates in the system of equations to reduce the number of deflections to be measured. In this procedure, the equations of the system are solved one by one. In this way, once an unknown area is calculated from the equilibrium equation of one of its nodes, this area might contribute to solve new unknowns in the equilibrium equations of other nodes. For example in the case of the continuous beam in Fig. 2, when u_1 is measured, A_1 can be obtained from (1) of Fig. 1. Then, calculated A_1 and measured u_2, they can be used to obtain A_2 from (2) of Fig. 1. Finally, calculated A_2 and measured u_3, they can be used to obtain A_3 from (3). This very simplified example shows that A_1, A_2 and A_3 can be obtained by measuring deflection in three conveniently selected nodes (u_1, u_2 and u_3). This way of solving the system of equations illustrates the recursive process of the observability analysis and it represents the concept of observability flow.

In the structure presented in Fig. 2, an observability flow (flow 1) is initiated in Eq. (1) when A_1 is calculated. Then, the observability flows towards the rest of equations and the new areas are successively calculated. To enable the calculation of an estimate from the observability flow, it is necessary to connect conveniently the tree branches. With this aim, the branches must include information that (together with the calculated estimates) can be used to solve new equations. The observability flow 1 is represented in the right hand side of the equations of the axial resistant mechanism, in the main diagonal of the stiffness matrix and in the axial observability tree, T_N, by a continuous arrow in Fig. 2. The required measurement set obtained by the flow consists of u_1, u_2 and u_3. The observed estimates are colored in green color. An alternative observability flow (flow 2) might be initiated when A_3 is obtained from Eq. (4) after introducing the measured vale u_4. In this case, to observe all cross sectional areas it is necessary to measure an alternative set of deflections (u_4, u_3 and u_2). The observability flow 2 is represented by a dashed arrow in Fig. 2.

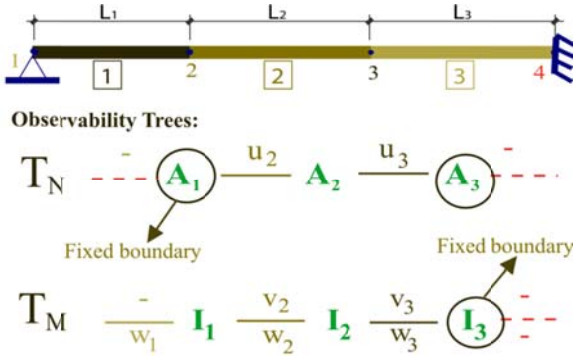

Fig. 3 T_N and T_M with boundary conditions

The boundary conditions reduce the points of the structure where deflections and/or rotations might be measured to introduce information to the system. To illustrate how to include the boundary conditions into the representation of the observability trees the example in Fig. 3 is presented. This structure is the same as that in Figs. 1 and 2 but includes the boundary conditions in edged nodes. Node 1 has the vertical and the horizontal deflection fixed while in node 4 all the movements are fixed. A circle is used to represent the fixed boundary conditions at the tree node. This circle is added only in those cases where the boundary conditions are such that no information might be obtained from one equation of the stiffness matrix method. That equation is represented in an edged branch. In the case of the T_N tree, the first and the third node, A_1 and A_3, are circled because the corresponding equations of edged branches do not introduce any information to the system. This is clearly appreciable in Eqs. (1) and (4) of the axial resistant mechanism in Fig. 2. In these cases, as the boundary conditions impose a null horizontal deflection at nodes 1 and 4, Eqs. (1) and (4) cannot be used to obtain estimates. This lack of information is represented by a disconnection in the corresponding edged branches of T_N in Fig. 3.

The effects of the boundary conditions in the bending resistant mechanism of the continuous beam are also illustrated in Fig. 3. In this case, the branches of the T_M tree include information of two different equations (equilibrium of vertical equations and moments). For this reason, and despite the fact that the vertical deflection is fixed at node 1, its first tree node, I_1, is not circled because the first branch might still introduce useful information to the system of equations by mean of w_1. A different thing happens in the third tree node, I_3. In this case, the equation associated with the last branch is useless because v_4 and w_4 are forced to be zero by the boundary condition. To indicate this fact in the observability tree, the I_3 is circled and the last branch is disconnected.

To understand the observability trees, different beam structures are analyzed in Example 1.

2.1 Example 1: Beam

The first analyzed structure corresponds with the horizontal beam presented in Fig. 4. Its FE model includes 5 nodes and 4 bars L_1, L_2, L_3 and L_4 long, respectively. Two intermediate nodes (nodes 6 and 7) are also considered. The applied nodal loads correspond to those introduced in the static load test. All the beam elements have the same known E. Nevertheless, both their area, A_j, and their inertia, I_j (framed and numbered from 1 to 4 in Fig. 4) are assumed unknown. This implies that 8 unknown estimates (A_1 to A_4 and I_1 to I_4) must be identified. Horizontal deflections

(u), vertical deflections (v), rotation (w), horizontal reactions (H), vertical reactions (V), and moments (M) followed the positive direction of axes presented in Fig. 4.

The observability of the unknown estimates in eight different measurement sets (cases 1.1 to 1.8) is summarized in Fig. 4. Differences between the analyzed cases refer to the beam inclination, α_j, (horizontal beam, $\alpha_j=0$, in cases to 1.1 to 1.6 and inclined beam, $\alpha_j\neq0$, in cases 1.7 and 1.8) and to the boundary conditions (simply supported in cases 1.1 to 1.3 and clamped-supported in cases 1.4 to 1.8). For each case, Fig. 4 summarizes the measured deflections introduced into the observability analysis (left hand side) and the axial (T_N) and flexural (T_M) observability trees (right hand side). In the observability trees, observed parameters are in bold green color. Unobserved parameters are in italics red color. Circled nodes indicate restrictions by boundary conditions. Green arrows show the observability flow through the recursive process. Dashes in branches (disconnected branch) indicate that no information is measured in the corresponding node of the FEM.

Cases 1.1 to 1.3 correspond with a horizontal and simply supported beam. In case 1.1, 8 measured deflections and rotations (w_1, u_2, v_2, u_3, v_3, u_4, v_4 and u_5) are introduced into the observability analysis. In this case, all the variables can be observed. On the one hand, the T_N observability tree shows that all the areas are observed after an observability flow (initiated in A_4) flows from right to left in the tree. On the other hand, the T_M observability tree shows that the inertias can also be observed. In the initial observability analysis (number of recursive Step i=1), the location of the measurements in beam element 1 enables the observation of I_1 and an observability flow is initiated. As the branches of the tree are conveniently connected the observability flows from left to right and the rest of inertias can be successively observed in three more steps. The observed parameters throughout the recursive process are summarized in Table 1. It is important to highlight that the number of observed variables in each recursive step, $N.obs_i$, presented in this table includes not only areas and inertias, but also unknown deflections. Case 1.2 shows that all areas and inertias but A_4, I_3 and I_4 are observed when five deflections (u_2, v_2, u_3, v_3 and u_4) and one rotation (w_3) are measured. The T_N observability tree shows a disconnection (discontinuous red line) in edge branch as no horizontal deflection is measured at node 5. This illustrates that A_4 cannot be observed unless u_5 is measured. The T_M observability tree shows how the flow can be initiated at an inner node (I_2) and to flow to edge nodes when adequate connectivity is provided. Nevertheless, when adjacent nodes of the tree are not conveniently connected, (e.g. when neither vertical deflection nor rotation in node 4 is measured) the observability cannot flow. This is the case of the right hand side of T_M in which, I_3 and I_4 cannot be observed. In case 1.3, A_3, A_4, I_1 and I_4 can be observed when five deflections (v_2, u_3, u_4, v_4 and u_6) and two rotations (w_2 and w_5) are measured. This example shows that separated parts of the trees can be observed when a branch is disconnected. The T_M tree illustrates that different observability flows can be initiated at different parts of the structure when requirements to initiate the flows are adequately satisfied. Nevertheless, when a branch is disconnected, the mechanical properties of the adjacent nodes of the trees (such as A_1, A_2, I_2 and I_3) cannot be observed.

Cases 1.4 and 1.5 correspond to a horizontal clamped-supported beam. This beam is statically indeterminate in the axial and flexural resistant mechanism. In case 1.4, neither any A nor I can be observed when 7 deflections and rotations (u_2, v_2, u_3, v_3, u_4, v_4 and w_5) are introduced. In the T_N observability tree, the absence of observed areas can be explained by the fact that no observability flow can be initiated. The analysis of the T_M indicates that an additional condition arises in clamped-supported beams. In these structures, the observability of the inertia that connects the clamped node (I_1 in this case) is compulsory. To observe this inertia, it is necessary to relocate the

measured deflections. In this way, defections might be measured at the proximities of the clamped edge at an intermediate point of the beam. This is illustrated in case 1.5, where w_5 is substituted to the vertical deflection at the intermediate node 7. The horizontal deflection u_7 is also introduced. A summary of the observed parameters throughout the recursive process in case 1.5 is presented in Table 1.

Unlike horizontal and vertical beams, the axial and flexural structural behavior of inclined beams ($\alpha_j \neq 0$) cannot be treated independently unless the horizontal and vertical forces and the deflections can be determined in the local axes of the beam. In simple structures, forces and deflections in global axes (e.g. determined by topography) can be projected into local axes of the beam. Nevertheless, in structures with a large number of elements with different local axes, this change of axes is discouraged. For this reason, this section analyzes the effects of the inclination of the beam when measurements in global axes (u_k and v_k). In this case, both deflections include information of both resistant mechanisms and therefore, the observability flow can only be represented by a common observability tree, called $T_{N\text{-}M}$. This tree links the axial (T_N) and flexural (T_M) structural behavior of the beam.

To illustrate the peculiarities of the $T_{N\text{-}M}$ observability tree, cases 1.6 to 1.8 are analyzed. The beam used in these cases only differs with that presented in cases 1.4 and 1.5 in the fact that it has an inclination α. In case 1.6, all the estimates are calculated when 8 deflections (u_2, v_2, u_3, v_3, u_4, v_4, u_7 and v_7) are measured. The $T_{N\text{-}M}$ observability tree shows that, thanks to the information measured at the intermediate node 7, observability flows are initiated in both resistant mechanisms (at nodes A_1 and I_1). The connectivity of the branches of the tree enables the observability of all the estimates. This observability flow corresponds with the sum of the separated observability flows for the equivalent horizontal beam presented in case 1.5. In the following case, a disconnection in the horizontal deflections is introduced at the branch joining the mechanical characteristics of the beam elements 2 and 3 (v_3). The analysis of the observability tree of these two cases shows that in inclined beams a disconnection at any resistant mechanism also affects the observability of the other one. A summary of the observed parameters throughout the recursive process in case 1.7 is presented in Table 1. Finally, in case 1.8, no area can be observed because no observability flow can be initiated. Furthermore, as the node 1 is clamped, the observability of beam 1, I_1, is compulsory. Nevertheless, the disconnection of the branch that connects structural parameters in bars 1 and 2 (u_7) makes that any flexural stiffness can be observed.

Table 1 Number of observations ($N.obs_i$) including deflections, observed areas and inertias in cases 1.1, 1.5 and 1.7 throughout the steps (i) of the recursive process

	Case 1.1			**Case 1.5**			**Case 1.7**		
Step (i)	**$N.obs_i$**	**Areas**	**Inertias**	**$N.obs_i$**	**Areas**	**Inertias**	**$N.obs_i$**	**Areas**	**Inertias**
1	10	A_1 to A_4	I_1	12	A_1 to A_4	I_1	10	A_1, A_4	I_1
2	12	A_1 to A_4	I_1, I_2	14	A_1 to A_4	I_1, I_2			
3	14	A_1 to A_4	I_1, I_2, I_3	16	A_1 to A_4	I_1, I_2, I_3			
4	18	A_1 to A_4	I_1 to I_4	18	A_1 to A_4	I_1 to I_4			

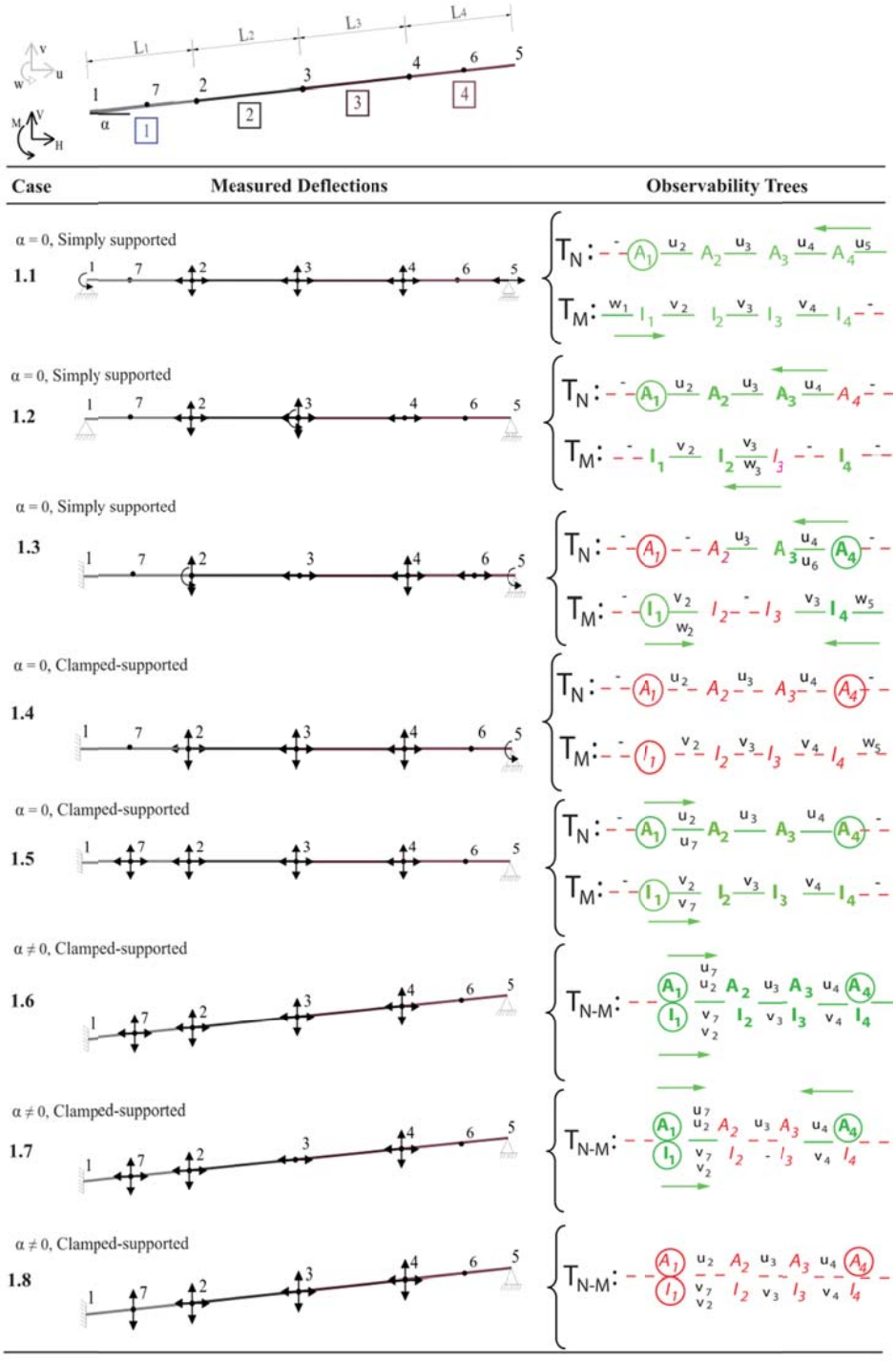

Fig. 4 Observability trees for cases in example 1. A_j and I_j in bold green colour are observed and in italics red colour are not

2.2 Algorithm

Input: Geometry, boundary conditions and unknown mechanical properties (N_I flexural and N_A axial stiffnesses).

Output: For each analysis direction (forward or backward), different sets of minimum measurements clustered in matrices $[M_F]$ and $[M_B]$ can be obtained. On the one hand, $[M_F]$ defines the required measurements obtained by a forward observability flow while $[M_B]$ defines those measurements obtained by a backward flow.

Step 1: Creating a FEM to be analyzed: From the geometry of the beam an adequate FEM is defined. This FEM includes nodes to separate the structural beam elements with different unknown mechanical properties and to represent the boundary conditions.

Step 2: Evaluating the flexural resistant mechanism from a forward direction[1]: The nodes are looked over from left to right. A vertical deflection or a rotation is available when the following two conditions are fulfilled: (1) The measurement is not null due to boundary conditions and (2) it has not been previously selected. The vertical deflection or the rotation of each node is selected when at least one of them is available. Else the vertical deflection or the rotation of the next node is selected if available. Otherwise, an additional node is created to measure either its vertical deflection or its rotation. The N_I selected values are saved in $[M_F]$.

Step 3: Evaluating the flexural resistant mechanism from a backward direction[2]: The nodes are look over from right to left. The vertical deflection or the rotation of each node is selected when at least one of them is available. Else, the vertical deflection or the rotation of the next node is selected if available. Otherwise, an additional node is created to measure either its vertical deflection or its rotation. These N_I selected values are saved in $[M_B]$.

Step 4: Evaluating the axial resistant mechanism from a forward direction[3]: The nodes are looked over from left to right. The horizontal deflections of each node are selected when they are available. Else, the horizontal deflection of the next node is selected if available. Otherwise, an additional node is created to measure its horizontal deflection. These N_A selected values are saved in $[M_F]$.

Step 5: Evaluating the axial resistant mechanism from a backward direction: The nodes are looked over from right to left. The horizontal deflections of each node are selected when they are available. Else, the horizontal deflection of the next node is selected if available. Otherwise, an additional node is created to measure its horizontal deflection. All these values are saved in $[M_B]$.

Step 6: Correction to substitute rotations for deflections[4]: If we want to define an alternative

---

[1]The N_I measurements required to define the N_I unknown flexural stiffnesses are selected to assure an adequate connectivity of the N_I tree nodes. In a horizontal beam these measurements might be both vertical deflections and rotations. To define the possible measurement sets, the structure is analyzed forwards (from left to right) and available measurements are selected.

[2]To define the N_I measurements the structure is analyzed backwards. In this way, the measurements are selected from right to left.

[3]The N_A measurements required to define the N_A unknown axial stiffnesses are selected to assure an adequate connectivity of the N_A tree nodes. In a horizontal beam these measurements correspond with horizontal deflections. To define these deflections the structure is analyzed forwards and available measurements are selected.

[4]This step is presented because usually the rotations are difficult to be measured in actual structures. For this reason, rotations might be replaced by vertical deflections.

measurement set without rotations, the rotations in matrices $[M_F]$ and $[M_B]$ are replaced by vertical deflections at their corresponding nodes if available, or at next node if available, or at an intermediate node. Otherwise, go to step 7.

Step 7: Correction in clamped-supported beams with different mechanical properties and without intermediate supports: If the structure is clamped-supported and it includes different mechanical properties without intermediate supports, the measurement set that does not start at the clamped node is replaced for the other measurement set. Otherwise, go to Step 8.

Step 8: Correction in doubled clamped beams with different mechanical properties and without intermediate supports: If the structure is doubled clamped with different mechanical properties and without intermediate supports, an additional measurement is required. This additional information might correspond with an extra vertical deflection or rotation at any available node or at any intermediate node. Otherwise go to step 9.

Step 9: Results report: The matrices $[M_F]$ and $[M_B]$ are provided.

It is noted that in both vertical and horizontal beams the axial and the flexural resistant mechanisms can be studied separately from the measurements provided by $[M_F]$ or $[M_B]$. Nevertheless, this is not the case of inclined beams with measurements in global axes as both resistant mechanisms have to be considered together.

The algorithm can be developed to take into account the 3D behavior of beam elements. In such a case, transverse flexural stiffness and torsional stiffness have to be identified. The number of unknowns will be increased by N_{TI} (unknown transverse flexural stiffnesses) and N_T (unknown torsional stiffenesses). To define the additional required measurements new analyses must be carried out from a forward and a backward approach. In the case of the transverse flexural mechanism, these analyses are equivalent to those presented in Steps 2 and 3 for the vertical flexural mechanism. On the other hand, the analyses of the torsional resistant mechanism are equivalent to those presented in Steps 4 and 5 for the axial resistant mechanism.

2.3 Application of the algorithm

The algorithm presented in the preceding section has been applied for measurement set selection in the simply supported beam presented in case 1.1. Five of the alternative measurement sets obtained by the algorithm are summarized in Table 2. This table includes the measurement sets in the Forward, $[M_F]$, and the Backward, $[M_B]$, analysis direction. As we are aiming to get measurement sets including rotations in order to compare with the results presented in Section 2.1, Step 6 of the algorithm is intentionally skipped. However, it is to highlight that measurement set four includes a practical application without rotation measurements.

Table 2 Alternative measurement sets obtained by the algorithm by the Forward, $[M_F]$, and the Backward, $[M_B]$, analysis direction

Set	$[M_F]$	$[M_B]$
1	$u_2, u_3, u_4, u_5, w_1, w_2, w_3, w_4$	$u_2, u_3, u_4, u_5, w_5, w_4, w_3, w_2$
2	$u_7, u_3, u_4, u_5, w_1, w_2, v_3, v_4$	$u_7, u_3, u_4, u_5, w_5, w_4, v_3, v_2$
3	$u_7, u_3, u_4, u_6, w_1, v_2, w_3, v_4$	$u_7, u_3, u_4, u_6, w_5, v_4, w_3, v_2$
4	$u_2, u_3, u_4, u_6, v_7, v_2, v_3, v_4$	$u_2, u_3, u_4, u_6, v_6, v_4, v_3, v_2$
5	$u_7, u_3, u_4, u_6, v_7, w_2, v_2, w_3$	$u_7, u_3, u_4, u_6, v_7, w_4, v_4, w_3$

Application of the algorithm to 2D structures is presented in the next section. The SSI using observability techniques might also be applied to 3D structures. Nevertheless, due to the high connectivity of all mechanical properties, the representation of the 3D observability trees is far from being intuitive. Hence, the essence of the observability trees method is lost.

3. Measurement set selection in cable-stayed bridges

The structural audacity and lightness of the current cable-stayed bridges make these structures very sensitive to static and dynamic loads in service (see Swenson 2012, Lozano-Galant and Turmo 2014a) and during construction (see Lozano-Galant *et al.* 2013b, 2014b and Lozano and Turmo 2014b). However, in many cases, especially for short and medium span bridges, dynamic behavior is not crucial, whereas the response under static loads is indeed.

The structural behavior of this kind of structures is much more complicated than that of continuous bridges because their structural behavior depends on the interaction of the deck, the pylon and the stay cables. As presented in Lozano-Galant *et al.* (2013a), this interaction is especially problematic in SSI by observability techniques.

Unless some simplifications are assumed, the interaction between the different loads bearing elements results in complex $T_{N\text{-}M}$ observability trees. In these trees the essence of the parametric method is lost as they are very difficult to be understood and far from being intuitive. To illustrate these complex trees in a cable-stayed bridge, Example 2 is analyzed. To uncouple the linkage produced by the stays a set of simplifications is advised. Furthermore, a set of guidelines to make observability trees in cable-stayed bridges is presented. Next, these guidelines are used to define the measurement set of cable-stayed bridges with few stay cables and different pylon-deck connections. The statistic analysis of the effectiveness of arbitrary measurement set selection is also analyzed in one of these structures. Finally, the measurement set selection of a large scale cable-stayed bridge is carried out.

3.1 Example 2: Cable-stayed bridge with inclined pylon

In this example the cable-stayed bridge with inclined pylon presented in Fig. 5 is analyzed. The bridge deck of this structure corresponds with the beam analyzed in Example 1. In this structure three stay cables are used to transfer the loads to the pylon. This element is L_5 high and with an inclination β. The Young's modula of all the elements of the structure are assumed as known. This assumption is introduced to deal with unknown areas and inertias instead of axial and flexural stiffnesses. Nevertheless, and without any lack of generality, the method is still applicable when Young's modula are assumed as unknown.

The observability trees of four measurements sets (cases 2.1 to 2.4) are presented in Fig. 5. In the first case, the mechanical properties (A and I) of the deck, the pylon and the stays are assumed as unknown. This produces a set of 16 unknown mechanical properties (from A_1 to A_8 and from I_1 to I_8). To observe these estimates a minimum set of 16 deflections is required. This set includes the measurement of deflections at intermediate points of the stay cables. Observed estimates throughout the recursive process are summarized in Table 3. A simplified $T_{N\text{-}M}$ observability tree (without the measurements in the branches) of this structure is presented in Fig. 5. This tree shows that the resistant mechanisms of all the elements are strongly linked. This linkage complicates the initialization of observability flows and the observability throughout the recursive process.

To disconnect the resistant mechanisms of the deck from those of the stays and the pylon, it can be assumed that the stays behave mainly with the axial resistant mechanism. This hypothesis is commonly used in the literature (see SETRA 2001) and it neglects the stay inertia (I_j=0). This assumption is followed in case 2.2, in which the number of unknown mechanical properties is reduced to 13 (from A_1 to A_8 and from I_1 to I_4 and I_8). To assure the observability of these elements a set of 13 deflections is required. As presented in the simplified observability tree of Fig. 5, the inertia of the stays has been removed. The parameters that can be observed throughout the recursive process are summarized in Table 3.

The manufacturing process of the stays provides high confidence of the stay axial stiffness. Furthermore, if required, cable sag effects can be included into E_j by mean of the equivalent Ernst's modulus (see Podolny and Scalzi 1986) that depends on the length of the stay, its weight and its force, F. Therefore, in practice, the axial stiffness EA of the stays is traditionally assumed as known. The effects of introducing this hypothesis into case 2.2 are analyzed in case 2.3. In this example the number of unknown parameters is reduced to 10 (from A_1 to A_4, A_8, from $I_1$to I_4 and I_8). To observe these parameters, the measurement of a minimum set of 10 deflections is required. Introducing the stay cable area as a known parameter into the observability analysis facilitates the representation of the observability tree of the structure as the resistant mechanisms of the deck and the pylon might be studied separately as presented in Fig. 5. The deck observability trees correspond with those of the equivalent horizontal beam described in case 1.5. The pylon observability tree corresponds with that of an inclined cantilever beam. In this case, because of the inclination, the resistant mechanisms cannot be separated. It is important to highlight that there are an infinite number of minimum measurement sets.

For example, in case 2.3 all the mechanical properties can also be observed when a different measurement set substituting v_2 for w_2 or w_3 is introduced.

An additional hypothesis that can be added to provide more freedom in the selection of the measurement set consists of including the stay force F. In this way, the stay cables can be substituted in the observability analysis by their corresponding forces in the stay-anchorage points. This situation is presented in case 2.4, where the stays are replaced by their axial forces F. To show that the stays do no longer appear in the observability analysis, they are highlighted by a dotted line. In this example, to observe all the unknown estimates a new measurement set might be used. Compared with that presented in case 2.4, this set enables to interchange the deflections at the top of the pylon (node 9 in Fig. 5) with those at another point of the pylon (such as node 8 in Fig. 5) providing more freedom to the measurement set.

When only the stay cable axial resistant mechanism is assumed, it is possible to link the stay force, F, with the axial stiffness of the stay, EA, and its elongation, ΔL, as follows

$$F = EA \cdot \Delta L. \tag{2}$$

This equation might provide additional information to the system in the following cases: (1) When F and the deflections in both stay-anchorage points are measured, the axial stiffness EA of the stay can be calculated. (2) When F, EA, the deformations of one stay-anchorage point and one of the deformations (u_k or v_k) of the other anchorage point are measured, the unknown deformation of the anchorage point can be calculated. This information might be useful to reduce the number of points in the deck where horizontal deflection must be measured. (3) When one of the stay-anchorage points corresponds with a boundary condition, F can be used to calculate the boundary reactions, as in the case of the backstays.

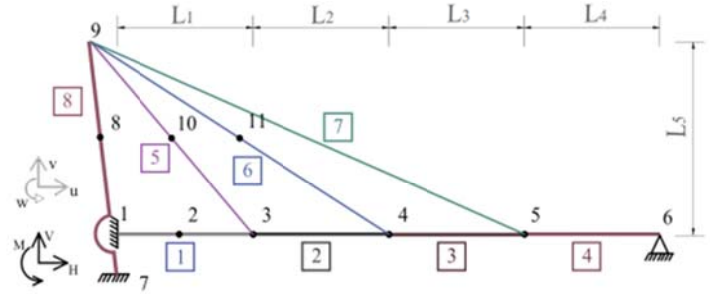

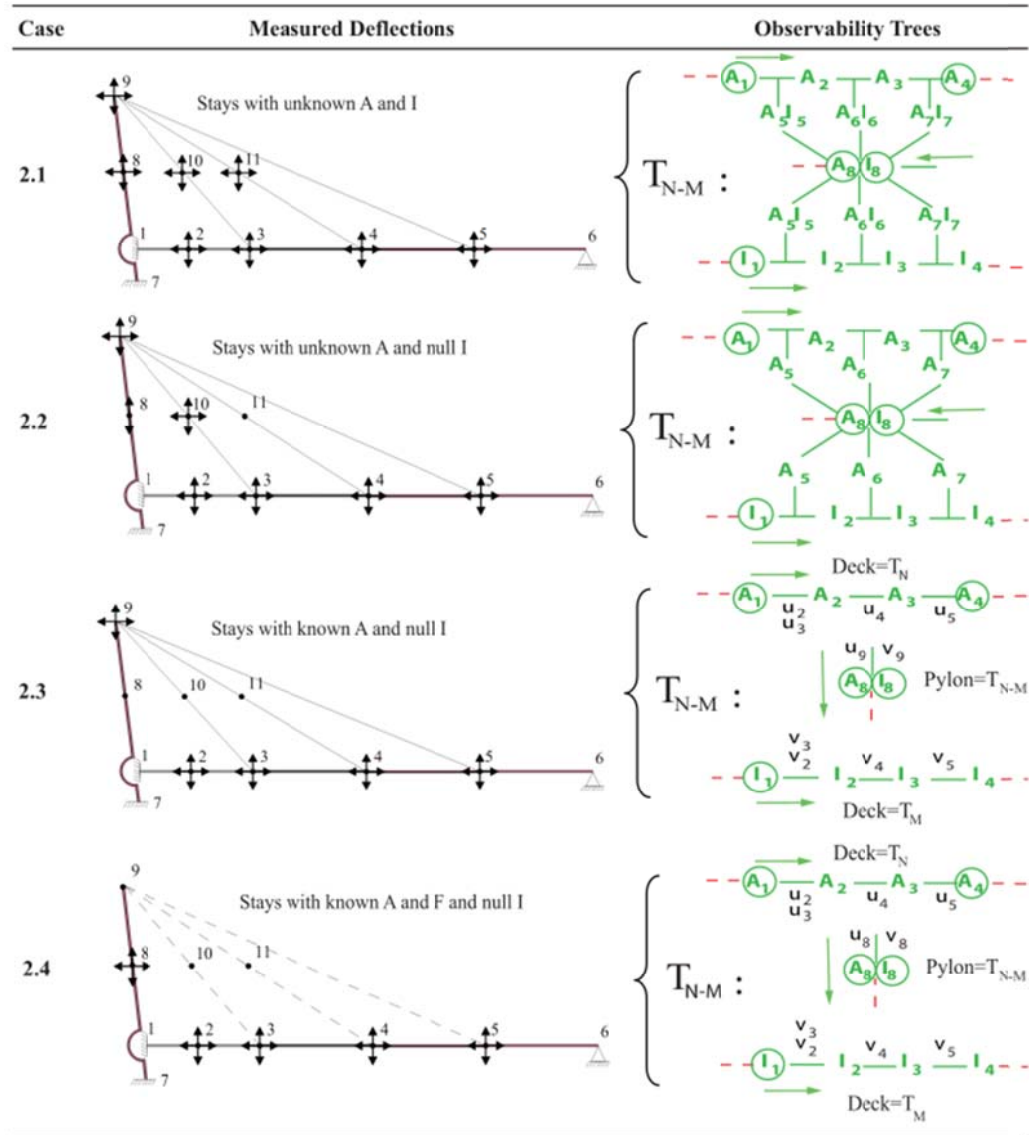

Fig. 5 Observability trees for cases in example 2. A_j and I_j in bold green colour are observed

Table 3 Number of observations ($N.obs_i$) including deflections, observed areas and inertias in cases 2.1 and 2.2 throughout their recursive steps (i).

	Case 2.1			Case 2.2		
Step (i)	$N.obs_i$	Areas	Inertias	$N.obs_i$	Areas	Inertias
1	18	A_1, A_4, A_5, A_6, A_8	I_1, I_8	22	A_1 to A_8	I_1, I_8
2	23	A_1, A_2, A_4, A_5, A_6, A_8	I_1, I_2, I_5, I_8	24	A_1 to A_8	I_1, I_2, I_8
3	31	A_1 to A_8	I_1, I_2, I_3, I_5, I_7, I_8	26	A_1 to A_8	I_1, I_2, I_3, I_8
4	35	A_1 to A_8	I_1 to I_8	28	A_1 to A_8	I_1, I_2, I_3, I_4, I_8

3.2 Guidelines in cable-stayed bridges

The analysis of a number of structures provides the following guidelines to determine the T_N and T_M observability trees in cable-stayed bridges:

(1) T_{N-M} trees in cable-stayed bridges with unknown mechanical properties in the stays: If the mechanical properties of the stays (A and/or I) are assumed unknown, the observability trees of the structures are far from being intuitive because the resistant mechanisms of all the elements (deck, pylon and stays) are linked (see cases 2.1 and 2.2). Furthermore, in this case the minimum number of required deflection usually includes deflections at both stay-anchorage points and at intermediate points of the stays.

(2) T_N and T_M trees in cable-stayed bridges with known mechanical properties in the stays: The resistant mechanisms of the deck and the pylon can be separated from those of the stays by neglecting the stay inertia (I=0) and assuming as known the area of the stay (see case 2.3). This simplification facilitates the representation and understanding of the observability trees of the structure. In this case, the set of measurements has to include deflections in both stay-anchorage points. The application of these hypothesis leads to the following ideas: Additional information can be obtained from the axial resistant mechanisms of the stays by Eq. (2). In cable-stayed bridges without pylon-deck connection, the observability trees of the pylon and the deck can be studied separately. In this case the deck can be analyzed as a beam and the pylon as a cantilever beam. Both elements include a different axial T_N, and a flexural, T_M, observability tree that might be coupled together depending on the element inclination. In cable-stayed bridges with pylon-deck connection, the observability trees of the deck and the pylon are linked at the connection.

(3) T_N and T_M trees in cable-stayed bridges without stay elements: When in addition to the mechanical properties of stays (A known and I=0), the axial forces of the stays, F, are included as data, the stays can be substituted in the observability analysis by the corresponding forces in the stay-anchorage points. In this case, most of the ideas referring to the representation of these trees presented in the above point are still applicable. Nevertheless, measuring F forces provides more freedom in the selection of the measurement set (as deflections in the stay-anchorage points are not required). Therefore, more intuitive observability trees can be obtained.

3.3 Application to cable-stayed bridges with few stay cables

To test the performance of the observability trees in the case of large structures, the asymmetric cable-stayed bridge presented in Fig. 6 is analyzed in this section. This structure is based on that described by Aboul-Ella (1990). The concrete cable-stayed bridge includes a 37.5 m high pylon, a 92 m long main span and a 25 m long back span. To illustrate the influence of the pylon deck

connection, two different structures (B_5 and B_4 in Fig. 6) are analyzed. The differences between both structures are as follows: (1) different number of stay cables, five stays for B_5 and four for B_4, and (2) different type of connection between the deck and the pylon, no connection in B_5, and vertically simply supported in B_4. Both structures are simulated by a FE model that includes 18 nodes. The main characteristics of the bridge are presented in Fig. 6.

In the analysis proposed in this section the following hypotheses are assumed: (1) In order to make a more general application, it is assumed that the deck could be cracked in the proximities of the stay cables. This assumption makes the use of different deck stiffnesses necessary. (2) To simplify the representation of the observability trees, and without losing any generality, the pylon is assumed to have constant mechanical properties. (3) Null flexural stiffness of the stay cables. (4) The stay axial stiffness is assumed as known. This simplification can be assumed because the variability of the stay material and cross section is significantly lower than in elements from decks and pylons made of concrete at early stages of the service life. Moreover, specific tests can be made to collect information about the real area and stiffness of the stays [Sumitro *et al*. 2002]. (5) In order to assimilate the axial and the flexural stiffnesses to the area and the inertia, the Young's modulus of all structural elements are assumed as known. This hypothesis is followed in most of the methods presented in the literature (see Abdo 2012). All these hypotheses produce a set of 20 unknown mechanical properties (from A_1 to A_{10} and from I_1 to I_{10}). (6) The structure is assumed to behave linearly during the non-destructive test and therefore, the effects of geometrical nonlinearities have been neglected. (7) Only static element parameters are required for the condition assessment of the structure. (8) No dynamic loads are applied and the structure is stiff enough to neglect effects of the dynamic properties in the static test. This is a reasonable assumption that can be applied to most of the medium span cable-stayed bridges no subjected to earthquake loads.

By following the guidelines provided in the preceding sections, the observability tree of B_5 results from the summation of those of two independent beams (a horizontal simply supported beam for the deck and a cantilever one for the pylon). One of the infinite number of minimum measurement sets, $B_{5\text{-}1}$, is presented in Fig. 7. In this set, the required deflections (u_1, u_2, u_5, u_6, u_7, u_9, u_{10}, u_{11}, u_1, u_{13}, u_{16}, v_2, v_4, v_6, v_7, v_8, v_9, v_{10}, v_{11} and v_{12}) are determined to provide adequate connectivity to the observability trees of the axial and resistant mechanisms of the structure. The observability flows obtained are presented in Fig. 7. This figure also includes three alternative measurement sets, $B_{5\text{-}2}$ to $B_{5\text{-}4}$, with the minimum number of measurements.

In structure B_4, due to the pylon-deck connection, the resistant mechanisms of the deck and the pylon are linked. This is appreciable in Fig. 8 where the corresponding $T_{N\text{-}M}$ observability tree is presented. In this case the area of the pylon, A_{10}, is linked with the inertia in the deck at the pylon connection, I_8, and the inertia of the pylon, I_{10}, is liked with A_8 and I_8, respectively. It is important to highlight that I_{10} includes a clamped node (node 16) and therefore, that inertia has been circled in the tree. Application of the guidelines presented in the preceding sections can be used to provide one of the sets with a minimum number of measurements. The set $B_{4\text{-}1}$, which is presented in Fig. 8, includes (u_1, u_2, u_3, u_4, u_5, u_6, u_8, u_9, u_{10}, u_{11}, u_{12}, u_{13}, v_3, v_4, v_6, v_7, v_9, v_{10}, v_{11} and v_{12}). Despite of the fact that an infinite number of alternative measurement sets can be defined, it is noted that the definition of these sets is not trivial at all. In fact, these measurements cannot be arbitrarily selected because they rarely provide adequate identification of the unknown variables. This fact is illustrated by the random analysis presented in the following section.

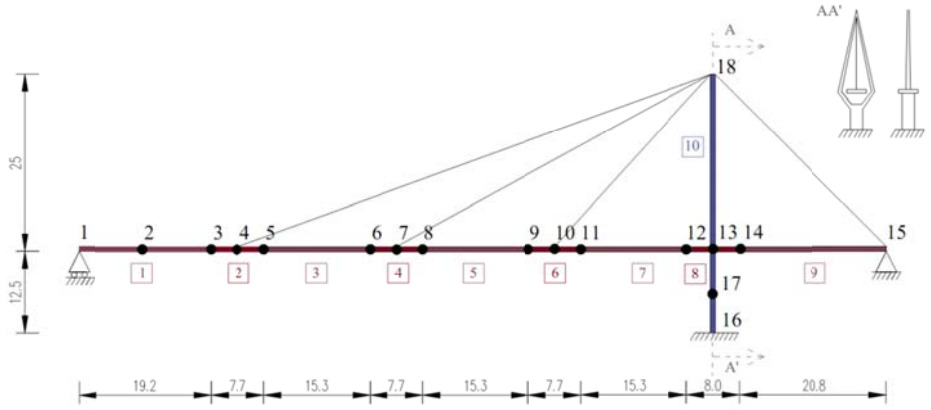

Fig. 6 Geometry and material properties (framed) of a cable-stayed bridge without, B_5, and with, B_4, pylon-deck connection. Units in m

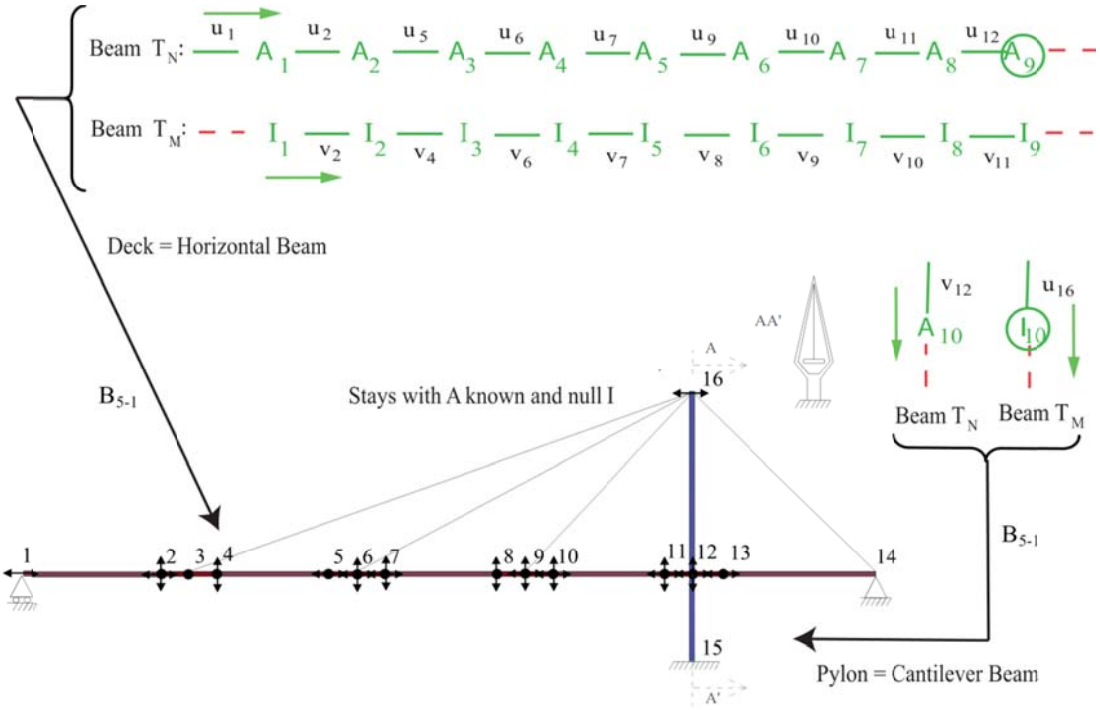

Minimum Measurement Set

Case	Measured u	Measured v
$B_{5\text{-}1}$	$u_1, u_2, u_5, u_6, u_7, u_9, u_{10}, u_{11}, u_{12}, u_{13}, u_{16}$	$v_2, v_4, v_6, v_7, v_8, v_9, v_{10}, v_{11}, v_{12}$
$B_{5\text{-}2}$	$u_1, u_2, u_3, u_4, u_6, u_7, u_8, u_9, u_{10}, u_{13}, u_{16}$	$v_2, v_4, v_6, v_7, v_9, v_{10}, v_{11}, v_{12}, v_{13}$
$B_{5\text{-}3}$	$u_1, u_3, u_4, u_5, u_6, u_7, u_8, u_9, u_{10}, u_{12}, u_{13}, u_{16}$	$v_4, v_6, v_7, v_9, v_{10}, v_{11}, v_{12}, v_{13}$
$B_{5\text{-}4}$	$u_1, u_2, u_4, u_5, u_6, u_7, u_8, u_9, u_{10}, u_{11}, u_{12}, u_{13}$	$v_3, v_4, v_5, v_7, v_8, v_9, v_{11}, v_{12}$

Fig. 7 Determination of different sets of minimum deflections ($B_{5\text{-}1}$ to $B_{5\text{-}4}$) from observability trees. Stays are assumed with known A and null I

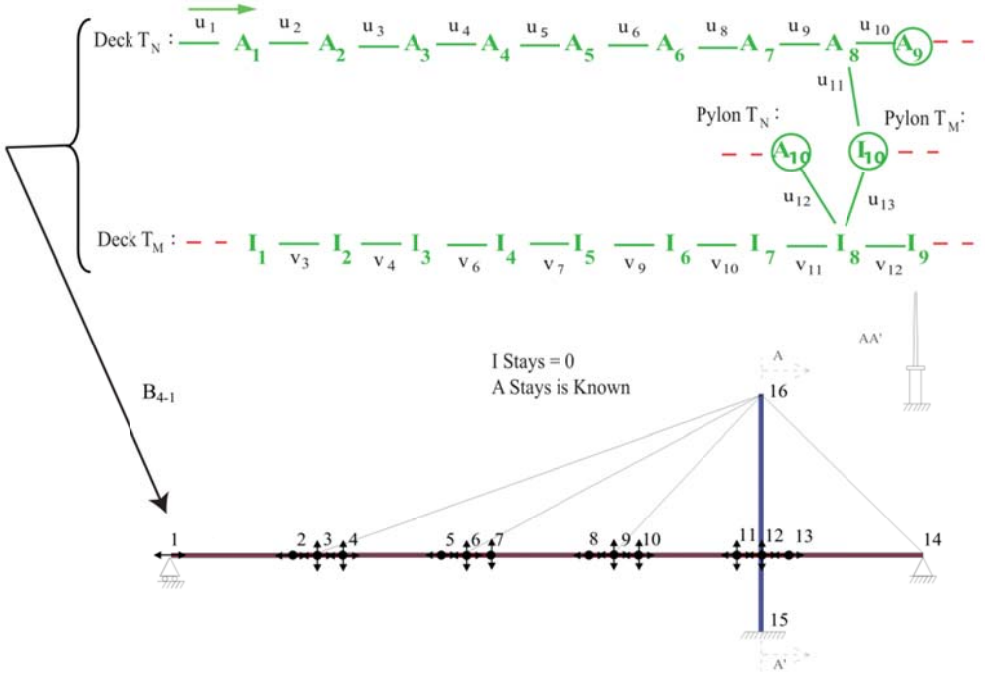

Fig. 8 Determination of measurement set in B_{4-1} from observability trees. Stays are assumed with known A and null I

3.4 Random set of measurements

In practice, the random selection of measurements is discouraged. Nevertheless, in this section the random selection is presented to prove that the selection of the measurement set is not as trivial as it might seem because the resulting system is not a linear one as polynomial equations appear. For this reason, in this section a statistical analysis is presented to evaluate the result of selecting measurement sets in an arbitrary way without using the guidelines that the use of observability trees provides. This analysis has been carried out for structure B_4 described in the preceding section.

To define all the unknown stiffness variables of this structure 20 deflections or rotations are required. In this case, 5.1×10^{11} combinations of different arbitrary measurements appear (42 possible measurements taken 20 at a time). These deflections and rotations are randomly selected from the degrees of freedom of the model nodes.

Fig. 9(a) shows the number of observed stiffness variables and the percentage of occurrence for the sets of 20, 25 and 29 arbitrary measurements. Fig. 9(b). shows the mean of observed stiffness variables for different number of selected measurements.

From the analysis of different sets of measurements randomly selected, the following points can be drawn:

- When the number of measurements is increased, the probability to identify all the unknown stiffnesses is increased.
- The possibility to achieve a full observability with only 20 measurements is 0.04%.

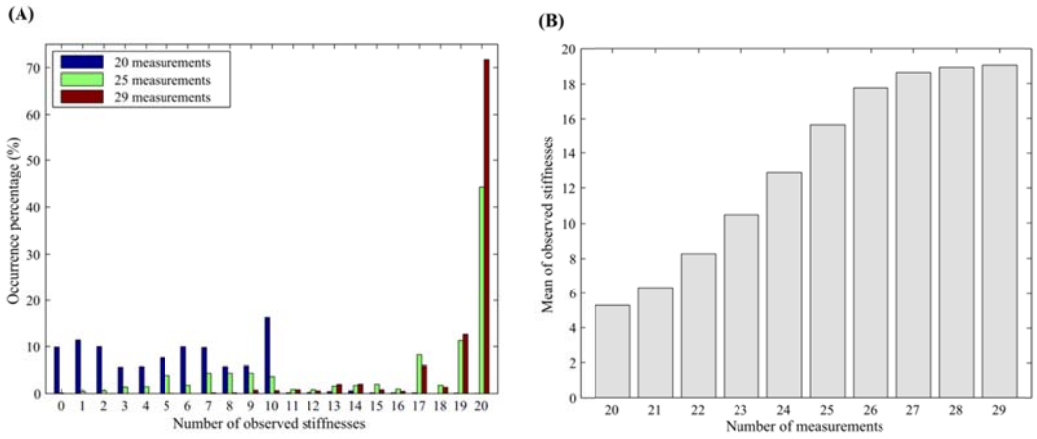

Fig. 9 Analysis of arbitrary measurement selection in B_4. (a) Occurrence percentage of observed stiffnesses, and (b) Mean of observed stiffnesses

- With 20 measurements, there is a probability of 10% of not observing any variable.
- 29 measurements (45% more than the minimum ones) are necessary to observe all the stiffness variables with a probability of 70%.
- With only 20 measurements, the mean of observed variables is almost 6.
- With 25 randomly selected measurements, the mean of observed variables is hardly 15.
- With 29 randomly selected measurements, the mean of observed variables does not achieve the full observability.

The results of this example show the importance of defining conveniently the type and location of the measurements by the observability trees. In fact, even higher measurement sets might not provide adequate SSI of unknown parameters.

3.5 Cable-stayed bridge

In this section, the SSI of the model of a cable-stayed bridge projected in the city of Wuxi (China) is analyzed. This bridge has a unique concrete pylon 60 m high, a concrete deck 180 m long and 18 stay cables. The analyzed FEM presents the following geometrical simplifications: stays have all the same cross sectional area and the deck is straight and has no camber. The geometry of this FEM is summarized in Fig. 10(a). This FEM is based on the same simplification hypotheses presented in Section 3.3. When these hypotheses are introduced a number of 61 nodes, 78 bars and 56 different mechanical properties (framed in Fig. 10(b)) appear.

The following additional simplifications have been carried out in the stay cables (elements from 39 to 56): (1) Known area. (2) Null inertia and (3) Measured forces in the static test F. These simplifications lead to a number of 76 unknown mechanical properties (A and I in elements from 1 to 38).

The SSI of this structure was analyzed by observability techniques in Lozano-Galant *et al.* 2014a. In this work a set of 99 deflections were required to identify all the unknown parameters. The definition of this measurement set was far from systematic as it was based on a trial and error analysis because at that time the potential of the recursive process was not completely understood. The observability trees might be used to reduce the measurement set to a minimum.

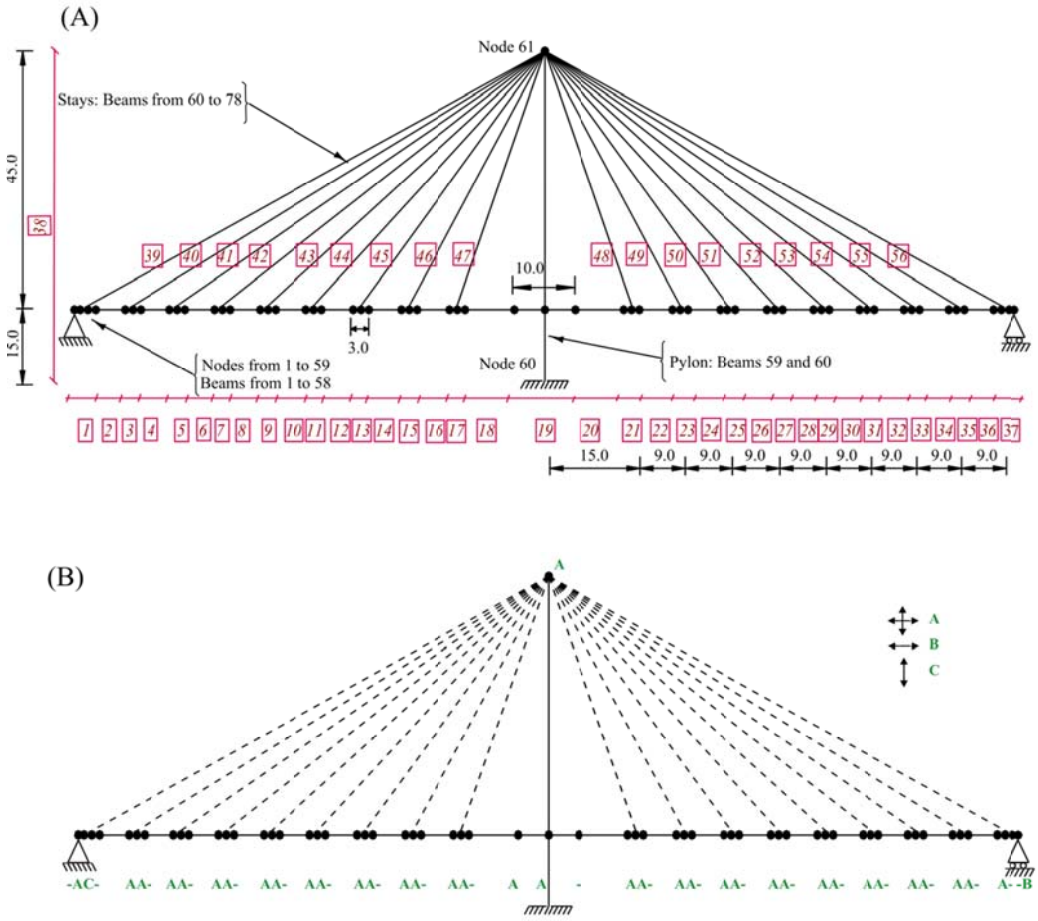

Fig. 10 Cable-Stayed bridge in Wuxi. (a) Geometry and mechanical properties, (b) Required deflections to be measured

One of the infinite possible sets with the minimum number of measurements is presented in Fig. 10(B). To facilitate its representation, in this figure the different deflections are named (A for u and v, B for u and C for v). This set was obtained by the algorithm described in Section 2.2. The shape of the tree is similar to that presented in Fig. 8. Nevertheless, the number of unknown variables discourages its graphical representation. The proposed measurement set initiates an observability flow at node 1 that flows to the right hand side of the structure in 75 recursive steps.

The comparison of the measurement sets obtained by both methods shows the convenience of using observability trees. In fact, the minimum measurement set (composed of 76 measurements) has only been achieved when the observability trees were used.

4. Conclusions

One of the most important steps in any Structural System Identification (SSI) method consists

on defining an adequate measurement set. Despite of its importance, the observability techniques presented in the literature propose the measurement set selection by trial and error. This lack of a systematic procedure for measurement set selection reduces significantly the applicability of the observability techniques. To fill this gap, this paper proposes a new and innovative method, the observability trees, for measurement set selection in SSI by observability techniques. This method also provides a deep understanding of the physical meaning and the necessity of each of the measurements.

The observability trees show graphically how the unknown estimates (such as bending stiffness, areas or inertias) are successively calculated throughout the recursive process of the observability analysis. These trees can be proved as a powerful tool for measurement set selection in beam bridges that can also be applied in complex structures, such as cable-stayed bridges. Nevertheless, in these structures, the strong link among structural parameters advises to assume a set of simplifications to increase the trees intuitiveness. In addition, a set of guidelines are provided to facilitate the representation of the observability trees in this kind of structures. These guidelines are applied in bridges of growing complexity that are used to explain how the characteristics of the geometry of the structure (e.g. deck inclination, type of pylon-deck connection, or the existence of stay cables) affect the observability trees. From these analyses, the following conclusions might be obtained. Firstly, in non-inclined decks the axial and the flexural observability trees can be independently analyzed. Observability trees of these structures can be analyzed independently as a disconnection in a structural mechanism does not affect the other one. On the contrary, in structures with inclined decks the axial and the flexural observability trees are coupled for gravity loads and they need to be studied together. Secondly, in cable-stayed bridges, the proposed simplifications enable the calculation of the measurement sets by the algorithm for beams. In these structures, the pylon-deck connection plays an important role in the geometry of the observability trees.

The importance of the observability trees is justified by a statistical analysis of measurement sets randomly selected. This study shows that, in the analyzed bridge, the probability of selecting an adequate measurement set with a minimum number of measurements at random is practically negligible. Furthermore, even higher measurement sets might not provide adequate SSI of the unknown parameters. Finally, to show the potential of the observability trees, a large-scale concrete cable-stayed bridge is also analyzed. The comparison with the number of measurements required in the literature by a trial an error procedure shows again the advantages of using observability trees.

Acknowledgements

The authors wish to thank the Ministerio de Economia y Competitividad (Spain) for the funding provided through the research project BIA2013-47290-R directed by Jose Turmo and founded with FEDER funds.

References

Abdo, M.A. (2012), “Parametric study of using only static response in structural damage detection”. *Eng. Struct.*, **34**, 124-131.

Aboul-Ella, F. (1990), "New iterative analysis of cable-stayed structures", *Comput. Struct.*, **40**(3), 549-554.
Adeli, H. and Jiang, X. (2006), "Dynamic fuzzy wavelet neural network model for structural system identification", *J. Struct. Eng.*, **132**(1), 102-111.
Arslan, M.E. and Durmus, A. (2013), "Construction stage effect on the dynamic characteristics of RC frame using operational modal analysis", *Comput. Concr.*, **12**(1), 79-90.
ASCE (2011), *Structural identification (st-id) of constructed facilities: approaches, methods and technologies for effective practice of st-id.* Technical report, ASCE SEI Committee on Structural Identification of Constructed Systems, American Society of Civil Engineers (ASCE).
Castillo, E., Lozano-Galant, J.A., Nogal, M. and Turmo, J. (2014), "New tool to help decision making in civil engineering", *J. Civil Engineering and Management.*, DOI: 10.3846/13923730.2014.893904.
Erdogan, Y.S. and Bakir, P.G. (2013), "Evaluation of the different genetic algorithm parameters and operators for the finite element model updating problem", *Comput. Concr.*, **11**(6), 541-569.
Joshua, L. and Varghese, K. (2013), "Selection of Accelerometer location on Brick Layers Using Decision Trees", *Comp.-Aided Civ. Inf.*, **28**(5), 372-388.
Lakshmanan, N., Raghuprasad, B.K., Muthurnani, K., Gopalakrishnan, N. and Basu, D. (2008), "Identification of reinforced concrete beam-like structures subjected to distributed damage from experimental static measurements", *Comput. Concr.*, **5**(1), 37-60.
Lee, J.W., Choi, K.H. and Huh, Y.C. (2010), "Damage Detection Method for Large Structures Using Static and Dynamic Strain data from Distributed Fiber Optic Sensor", *J. Steel Struct.*, **10**(1), 91-97.
Lozano-Galant, J.A., Nogal, M., Castillo, E. and Turmo, J. (2013a), "Application of observability techniques to structural system identification", *Comp.-Aided Civ. Inf.*, **28**(6), 434-450.
Lozano-Galant, J.A., Xu, D., Payá-Zaforteza, I. and Turmo, J. (2013b), "Direct simulation of the tensioning process of cable-stayed bridges", *Comput. Concr.*, **121**, 64-75.
Lozano-Galant, J.A., Nogal, M., Paya-Zaforteza, I. and Turmo, J. (2014a), "Structural system identification of cable-stayed bridges with observability techniques", *Struct. Infrastruct. E.*, **10**(11), 1331-1344.
Lozano-Galant, J.A., Ruiz-Ripoll, L., Payá-Zaforteza, I. and Turmo, J. (2014b), "Modifications of the stress-state of cable-stayed bridges due to staggered erection of their superstructure", *Baltic J. Road and Bridge Eng.*, **9**(4), 241-250.
Lozano-Galant, J.A. and Turmo, J. (2014a), "An algorithm for simulation of concrete cable-stayed bridges built on temporary supports and considering time-dependent effects", *Eng. Struc.*, **79**, 341-353.
Lozano-Galant, J.A. and Turmo, J. (2014b), "Creep and shrinkage effects in service stresses of concrete cable-stayed bridges", *Comput. Concr.*, **13**(4), 483-499.
Ni, Y.Q., Zhang, P., Ye, X.W., Lin, K.C. and Liao, W.Y. (2011), "Modeling of temperature distribution in a reinforced concrete supertall structure based on structural health monitoring data", *Comput. Concr.*, **8**(3), 293-309.
Meo, M. and Zumpano, G. (2005), "On the optimal sensor placement techniques for a bridge structure", *Eng. Struct.*, **27**(10), 1488-1497.
Podolny, W. and Scalzi, J.B. (1986), *Construction and design of cable-stayed bridges*. 2nd ed. New York: John Wiley & Sons.
Pothisiri, T. and Hjelmstad, K.D. (2002), "Strategy for finding a near-optimal measurement set for parameter estimation from modal response", *J. Sound Vib.*, **257**(1), 89-106.
Raich, A.M. and Liszkai, T.R. (2012), "Multi-Objective Optimization of Sensor and Excitation Layouts for Frequency Response Function-based Structural Damage Identification", *Comp.-Aided Civ. Inf.*, **27**(2), 95-117.
Sanayei, M., Onipede, O. and Babu, S.R. (1992), "Selection of Noisy Measurement Locations for Error Reduction in Static Parameter Identification", *AIAA J.*, **30**(9), 2299-2309.
Sanayei, M. and Saletnik, J. (1996), "Parameter estimation of structures from static strain measurements. I-formulation", *J. Struct. Eng. - ASCE*, **122**(5), 555-562.
Sanayei, M., Imbaro, G.R., McClain, J.A.S. and Brown, L.C. (1997), "Structural Model Updating Using Experimental Static Measurements". *J. Struct. Eng. - ASCE*, **123**(6), 792-798.
S.E.T.R.A. (2001), *Haubans. Recommandations de la Commission Interministérielle de la Précontrainte*,

Service d'Etudes Techniques des Routes et Autoroutes, France.
Sumitro, S., Jarosevic, A. and Wang, M.L. (2002), "Elasto-Magnetic Sensor Utilization on Steel cable-stress measurement", *Proceedings on the 1st fib Congress*.
Swensson, H. (2012), *Cable-stayed bridges*. Ernst & Sohn Gmbh and Co.
Turker, T., Bayraktar, A. and Sevim, B. (2014), "Vibration based damage identification of concrete arch dams by finite element model updating", *Comput. Concr*., **13**(2), 209-220.
Ubertini, F., Gentile, C. and Materzzi, A.L. (2013), "Automated modal identification in operational conditions and its application to bridges". *Eng. Struct*., **46**, 264-278.
Zhang, J.Y. and Oshaki, M. (2011), "Force identification of prestressed pin-jointed structures", *Comput. Struct*., **89**(23-24), 2361-2368.

CC